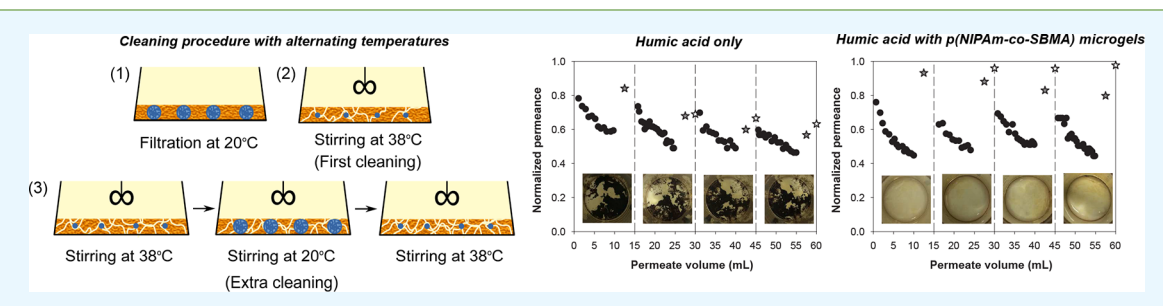


Canan Aksoy, Papatya Kaner, Ayse Asatekin, and P. Zeynep Çulfaz-Emecen*,

ACS APPLIED MATERIALS

& INTERFACES

^{*}Chemical and Biological Engineering, Tufts University, Medford, Massachusetts 02155, United States



ABSTRACT: In this study, we show that codeposition of temperature responsive microgels in the foulant cake layer and cleaning of the cake upon stimuli-induced size change of the microgels is an effective method of fouling removal. Humic acid in CaCl₂ solution was used as a model foulant and poly(n-isopropylacrylamide) (p(NIPAm)) and poly(n-isopropylacrylamide-cosulfobetainemethacrylate) (p(NIPAm-co-SBMA)) were used as temperature responsive microgels. Filtrations were done below the lower critical solution temperature (LCST) and temperature was increased to above the LCST for cleaning. As an extra cleaning a temperature swing of above, below and then again above the LCST was applied. P(NIPAm) was found to be ineffective in cleaning the foulant deposit despite the 20-fold change in its volume with temperature change at LCST. P(NIPAm-co-SBMA) microgels, on the other hand, provided high fouling reversibility on hydrophilic poly(ether sulfone)(PES)/poly(vinylpyrrolidone) (PVP) and hydrophobic PES membranes. Better fouling reversibility with these microgels was observed at low and high solution ionic strength. While the use of microgels alone increased fouling reversibility to some extent, even in the absence of temperature stimulus, 100% reversibility could only be obtained when a temperature switch was applied in the presence of microgels, showing the effect of microgels' volume change in cleaning.

KEYWORDS: stimuli responsive polymer, microgel, fouling reversibility, cake fouling, zwitterion, sulfobetaine

INTRODUCTION

Membrane fouling is the most important bottleneck of membrane filtrations in aqueous media. Membrane productivity and lifetime are directly related to the course and cleanability of fouling. Fouling can occur inside membrane pores or on the membrane surface. It may result from adsorption on the surface due to attractive interactions between filtered materials and the membrane surface, blocking the membrane pores with filtered materials, or from cake formation on the membrane surface, which is the result of an imbalance between permeate drag toward the membrane surface and back diffusion, causing deposition of filtered materials on the surface.^{1–4}

A variety of chemistries have been explored to render membrane surfaces resistant to foulant adsorption. Modification of the surface is achieved through blending of antifouling additives in the membrane during preparation, 5-10 grafting of antifouling groups after preparation, 11-13 or fabricating membranes from polymers consisting of antifouling groups. 14-18 This approach decreases fouling and the resulting flux decline during filtration which is due to adsorption and typically renders fouling more reversible.

In dead-end and feed-and-bleed type filtration configurations, which are often preferred with feeds of low foulant load because they are less costly compared to cross-flow filtration, a cake layer always forms on the membrane. In addition, in some membrane applications, such as Membrane Bioreactors (MBRs), the solid load in the feed is extremely high and cake fouling is unavoidable. 19-23 In such processes, while antifouling surface modifications are useful to some extent, after a certain amount of buildup, complete cake removal is not possible and irreversible fouling occurs. In this case, a cleaning procedure is applied to remove cake layers from the membrane surface. Physical cleaning can be done through a number of different ways. Forward flushing or relaxation involves stopping the driving force toward the membrane while maintaining cross-flow or air sparging, which loosens the cake layer. 24-28 In backwashing, the flow direction is reversed which pushes back the cake $^{26,2\%,29,30}$ and air sparging uses the wakes behind air bubbles to scour the membrane surface. 31–33 Addition of inorganic particles in the feed has also been shown to render cake fouling on membranes more reversible. 34-36 The particles added typically have two effects: The first is to decrease the compressibility of the cake

Received: February 20, 2019 Accepted: May 6, 2019 Published: May 6, 2019



[†]Middle East Technical University, Chemical Engineering Department, Ankara 06800, Turkey

and to render it more easily removable, where the added particles act as inert components within the cake layer, and the second is to adsorb organic components in the feed, which increases rejection and decreases internal fouling.

In this study we use stimuli-responsive polymeric microgels by adding them into the feed to the membrane before filtration, and we use the response of the microgels, which deposit within the cake layer on the membrane, to remove cake fouling from the membrane surface (Figure 1). Stimuli-responsive polymers have

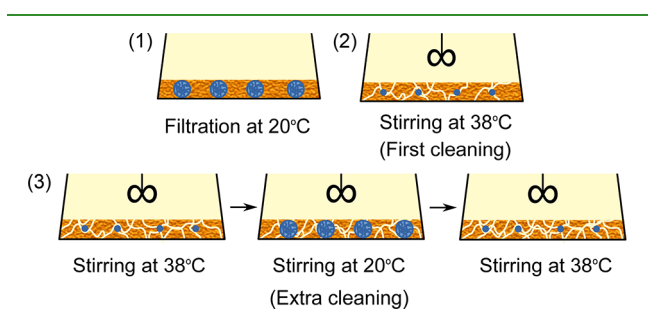


Figure 1. Schematic drawing of the filtration and cleaning procedure. The orange film represents the humic acid deposit, and the blue circles represent the microgels in swollen form (at 20 °C) or collapsed form (at 38 °C). Step (2) represents the first cleaning, and step (3) represents the extra cleaning procedure.

previously been used on membrane surfaces for pore size tuning³⁷⁻⁴⁷ and for fouling removal either by grafting the polymers to existing membrane surfaces, 48-54 fabricating the membranes from polymers with responsive side chains, blending responsive polymers into the membrane during fabrication, 57,58 or depositing them on the surface. 59,60 Temperature was used as the most common stimulus, and poly(nisopropylacrylamide), p(NIPAm), was the most commonly used temperature-responsive polymer to be tested for its ability to remove foulant layers upon its size change with temperature. 49-51,53-55,60 Membrane surfaces with p(NIPAm) chains have been shown to effectively clean protein, \$1,53-55,60 natural organic matter, \$3,55 and oil 49 deposits upon cleaning with alternating temperatures below and above the lower critical solution temperature of the polymer. Ionic strength, 48,51,52 light, 56,59 electrical potential, 57 and solvent 88 responsive membranes have also been cleaned upon stimulus response after being fouled by various types of foulants. As a different approach, Yu et al. 61 have infiltrated temperature-responsive poly(n-isopropylacrylamide) into the protein fouling layer previously formed on a membrane and changed temperature to change the volume of the polymer inside the protein deposit in order to remove the fouling layer.

Co-deposition of microgels within the foulant cake layer during filtration, where the effect of the microgels upon stimuli can extend to distances far from the membrane surface, is a novel approach for removing thick foulant deposits on membrane surfaces. A second advantage of this approach is that it can be implemented to existing, established membrane systems without the need for replacing the membrane. For this purpose, we used the thermoresponsive polymer poly(*n*-isopropylacrylamide) and poly(*n*-isopropylacrylamide-co-sulfobetaine methacrylate) copolymer which is responsive to temperature and ionic strength. Here, we report the effects of incorporating the two polymers cross-linked as microgels into the feed under a variety of conditions and using hydrophilic and hydrophobic membranes. We show that using a cleaning regime that involves

exposing the cake layer to warm water, or exposing it alternately to warm, cold, and warm water, can lead to highly enhanced removal of humic acid cakes without the need for a backwash.

EXPERIMENTAL SECTION

Materials. N-Isopropylacrylamide (NIPAm, 97%), N,N'methylenebis(acrylamide) (BA, 99%), potassium persulfate (KPS), ([2-(methacryloyloxy)ethyl]dimethyl-(3-sulfopropyl)ammonium hydroxide (sulfobetaine methacrylate, SBMA, 97%), poly(ethylene glycol) (PEG400, MW = 400 Da), poly(vinylpyrrolidone) (PVP K90 and K30), humic acid (sodium salt), calcium chloride dihydrate (≥99%), hexane (≥95%), toluene (≥99.5%), and dimethyl sulfoxide (≥99.5%) were purchased from Sigma-Aldrich. Poly(ethersulfone) (PES E6020P) was supplied by BASF.

Microgel Synthesis and Characterization. P(NIPAm) and P(NIPAm-co-SBMA) microgels were synthesized by free radical precipitation polymerization. In Table 1, amounts of monomers (NIPAm and SBMA), cross-linker (BA), and initiator (KPS) used in synthesis are given.

Table 1. Compositions of Microgel Synthesis Media as gr Reactant in 100 mL Water

microgel	NIPAm	SBMA	BA	KPS
p(NIPAm)	0.89		0.05	0.06
p(NIPAm-co-SBMA)	0.89	0.23	0.05	0.06

Before synthesis, monomers were purified by dissolving them in toluene and recrystallizing in hexane followed by filtration and drying. For p(NIPAm) synthesis, NIPAm and BA were first added in DI water, and the temperature was increased to 70 °C. Nitrogen was bubbled through the mixture to remove dissolved oxygen in water for 20 min, and then KPS was added to start polymerization. After 5 h, the reaction was stopped by quenching the reaction mixture. For p(NIPAm-co-SBMA) synthesis, SBMA monomers were added to the NIPAm-BA-KPS solution described above 15 min after KPS was added to start the polymerization reaction. After synthesis, microgels were separated from the mixture by centrifugation at 8000 rpm for 30 min, four times at 45 °C where polymers are in collapsed state, after which they were dried at room temperature.

Dynamic Light Scattering. Dynamic light scattering (DLS, Malvern CGS-3) analysis was performed in METU Central Laboratory. At each temperature, two to five measurements were taken using 0.01 g/L microgel suspensions.

Scanning Electron Microscopy. Membrane surfaces were observed by scanning electron microscopy (FE-SEM, QUANTA 400F) in METU Central Laboratory. Membrane cross sections were observed by Phenom G2 Pure Tabletop SEM in Tufts University. Membranes were dried under vacuum overnight and sputter-coated with Pd-Au before analysis. Pore size distributions and surface porosities were analyzed using ImageJ.

Membrane Fabrication. PES and PES/PVP blend membranes were fabricated by phase inversion. The polymer solution compositions used for fabrication were 25% PES, 20% PEG400-55% DMSO for the PES membranes and 15% PES, 5% PVP K90, 5% PVP K30-75% DMSO for the PES/PVP blend membranes. PEG400 in the PES membrane was used as pore former to obtain a comparable pore size distribution with the PES/PVP blend membranes. It is known from previous studies to leach out of the casting solution during coagulation such that the membrane prepared using PEG400 is a pure PES membrane. 62,63 The solution was cast at 250 μm thickness on a glass plate and coagulated in a water bath. The membranes were washed in water for 24 h and stored in 20% aqueous ethanol solutions until use.

Membrane Fouling. Pure water permeance and humic acid filtration (fouling) tests were done in a 50 mL Amicon cell without stirring. The absence of stirring was preferred to ensure that a comparable amount of material deposits on the membrane surfaces in each test where the same permeate volume is taken. 1 g/L humic acid-2

mM CaCl₂ solution was used as feed during fouling tests, as it is known that Ca²⁺ ions form complexes with humic acids and yield resistant fouling layers on the membrane. Filtration tests were done at 2 bar transmembrane pressure (TMP) and at room temperature, which was below the lower critical solution temperature (LCST) of the microgels. In cases where microgels were added to the feed, their concentration was 0.01 g/L. Forty mL of the solution was fed to the cell, and 10 mL of permeate was collected except when indicated otherwise. After filtration, hot water was added to the retentate side of the cell to bring the temperature to 38 °C. Cleaning was done at this temperature by stirring the retentate side in the cell for 5 min. In cases where an extra cleaning was applied, after this 5 min stirring at 38 °C, the retentate side was emptied and refilled with water at room temperature and stirred for 10 min, followed by emptying and refilling with water at 38 °C and stirring for another 10 min (Figure 1). The same cleaning procedure and temperatures were used in reference tests without the microgels. Humic acid concentration in feed, retentate, and permeate samples was measured by UV-visible spectroscopy (Shimadzu UV-1601) at 254 nm for rejection calculations.

Darcy's Law and resistances-in-series model was used to calculated the resistance due to foulant deposition on the membrane surface during filtration and the remaining resistance after cleaning. The viscosity of the permeate was taken as that of pure water at the filtration

The extent and reversibility of fouling was assessed by the decline and subsequent recovery in permeance, as well as the resistance due to fouling at the end of filtration and the reversible and irreversible fractions of this fouling resistance. While resistance analysis already takes into account changes in permeate viscosity at different temperatures, permeance values were similarly corrected for temperature.

RESULTS AND DISCUSSION

Characterization of Membranes and Microgels. SEM images of the surfaces of PES and PES/PVP blend membranes are shown in Figure 2(a) and (b). The pore sizes on the surfaces were measured as 21 ± 5 and 17 ± 6 nm for PES and PES/PVP blend membranes, respectively. Surface porosities were calculated as ca. 10% for the pure PES and ca. 6% for PES/ PVP blend membranes. On average the pure water permeance of PES membranes was $33 \pm 4 \text{ L/h} \cdot \text{m}^2 \cdot \text{bar}$, and that of PES/PVP

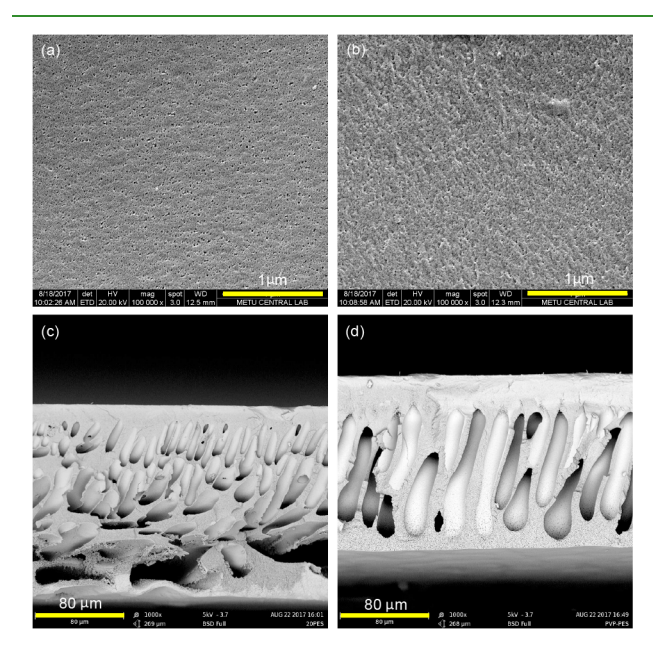


Figure 2. Surface and cross-section images of (a) and (c) PES and (b) and (d) PES/PVP blend membranes

membranes was $4.0 \pm 1.6 \text{ L/h} \cdot \text{m}^2 \cdot \text{bar}$. While the average pore sizes were similar, the difference in permeances can be attributed to the lower surface porosity of the PES/PVP blend membrane as well as the higher apparent skin thickness, which is taken as the thickness until the start of the macrovoids, seen in the SEM images (Figure 2(c) and (d)).

P(NIPAm) microgels showed LCST at 32 °C based on DLS measurements of hydrodynamic diameter (Figure 3), which is

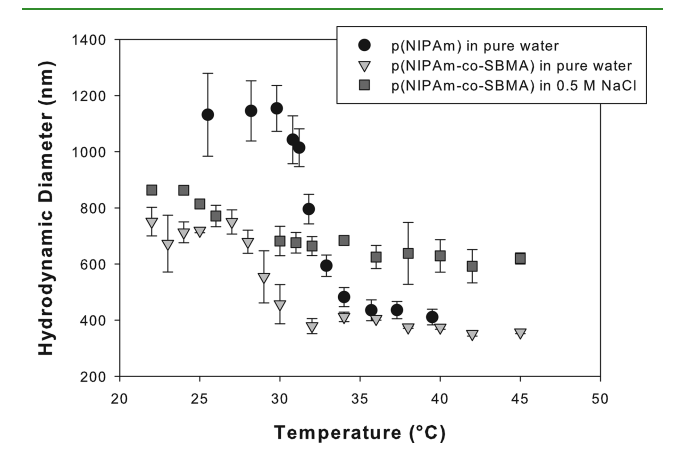


Figure 3. Hydrodynamic diameter as measured with DLS for p(NIPAm) and p(NIPAm-co-SBMA) microgels.

consistent with literature. 66-68 The diameters below and above the LCST were 1144 \pm 11 nm and 427 \pm 14 nm, respectively, roughly corresponding to a 20-fold increase in volume upon change in temperature.

p(NIPAm-co-SBMA) microgels showed LCST around 28 °C with diameters below and above the LCST as 721 ± 32 nm and 379 ± 25 nm, respectively (Figure 3), corresponding to about 7fold volume increase. The microgels were also ionic strength responsive, owing to the zwitterionic character of SBMA. At 20 $^{\circ}$ C, the diameter in 0.5 M NaCl increased to 864 \pm 7 nm, and at 45 °C, to 621 \pm 17 nm. The swelling occurred over a broader temperature range in the presence of salt and the volume change was only about 3-fold.

Effect of Microgels on Fouling Removal. The effect of microgel addition during filtration on the amount of fouling during filtration and reversibility of the foulant deposit was investigated in dead end filtrations followed by a cleaning step or multiple steps consisting of setting the retentate side of the membrane to the desired temperature and stirring for the predetermined time. Filtrations were done at room temperature, where the gels were in swollen form, and the first cleaning was done by increasing the temperature to above the LCST so as to collapse them. In extra cleaning, a second round of cooling and heating was applied to reswell and then reshrink the microgels that are within the foulant deposit. The humic acid rejection in all filtrations was $85 \pm 5\%$. The swollen-to-collapsed direction for cleaning was chosen based on preliminary experiments where it was observed that adding p(NIPAm) microgels to the feed in collapsed form aggrevated fouling on the membrane, possibly owing to the lower hydrophilicity of the gels above the LCST. ^{68,69}

P(NIPAm) Microgels with PVP/PES Blend Membrane. Figure 4 shows that when P(NIPAm) microgels were added to the humic acid feed solution during filtration, the permeance declined to 75% of the initial pure water permeance of the membranes. This decline was similar to the case where no **ACS Applied Materials & Interfaces**

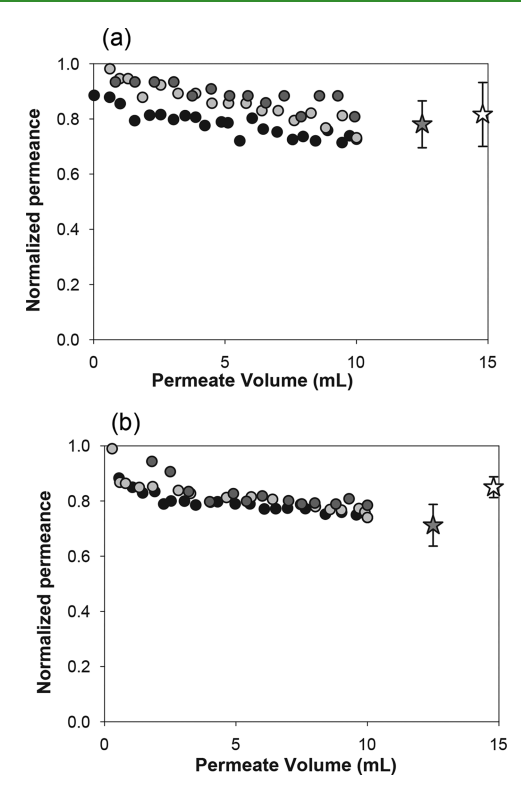


Figure 4. Normalized permeance as a function of permeate volume during humic acid filtration on PES/PVP blend membrane, circles represent data from three different membranes, gray stars show the average normalized permeance after the first cleaning, and white stars show the average normalized permeance after the extra cleaning: (a) No microgel and (b) 0.01 g/L p(NIPAm) added in the feed. Initial clean membrane pure water permeances are 3.5 ± 0.6 and 2.6 ± 0.1 L/h·m²·bar for (a) and (b), respectively.

microgel was used during filtration. After the first cleaning, which was done by increasing the temperature to 38 °C, above the LCST, the permeance was almost the same and after an extra cleaning consisting of decreasing the temperature below LCST and then increasing it back above LCST, the recovery in permeance was about 85% both with and without the microgels. Similar results were obtained when 10 times more PNIPAm (0.1 g/L) was added to the feed solution containing 1 g/L humic acid (data not shown). These results imply that, although p(NIPAm) experiences a very large volume change with temperature, this is not effective in removing the foulant deposit, possibly because of p(NIPAm)—humic acid interactions prevent the swelling of the microgel when inside the foulant deposit.

P(NIPAm-co-SBMA) Microgels on PVP/PES Blend Membrane. SBMA was incorporated into the microgels as a hydrophilic comonomer to decrease microgel—foulant and microgel—membrane interactions which was hypothesized to have diminished the swelling effect of p(NIPAm) microgels on removing the foulant layer. Effect of p(NIPAm-co-SBMA) microgels was tested by subjecting the same membrane to consequent filtration-cleaning-extra cleaning steps.

Figure 5 shows the normalized permeance of the PES/PVP blend membrane subjected to sequential filtrations followed by cleaning in three different cases. In Figure 5(a), no microgel was used. After the decline during filtration, the permeance could be recovered by up to 95% of the pure water permeance in the first filtration, and up to a similar percentage of the starting permeance in following filtrations. In consequent filtration

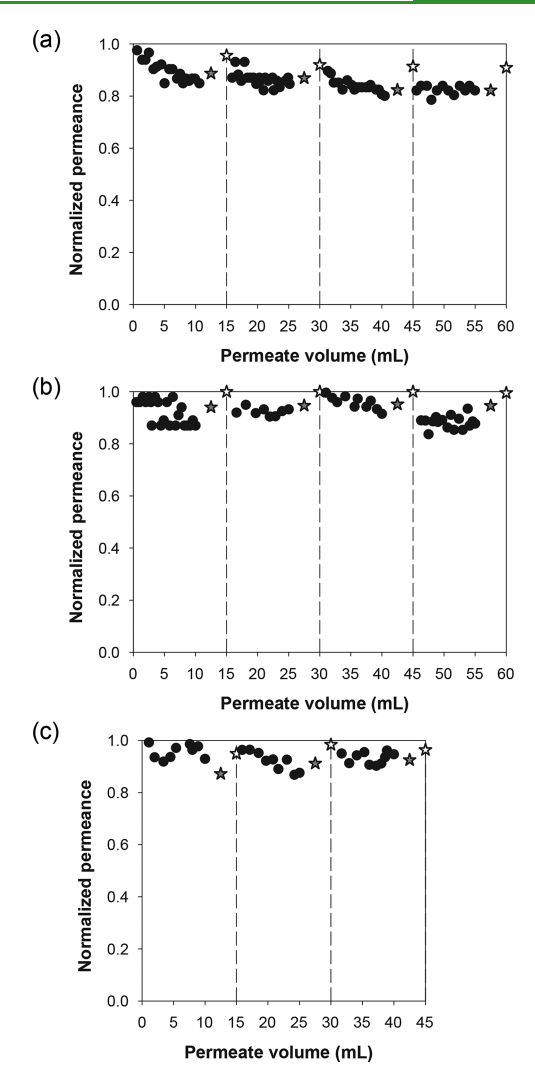
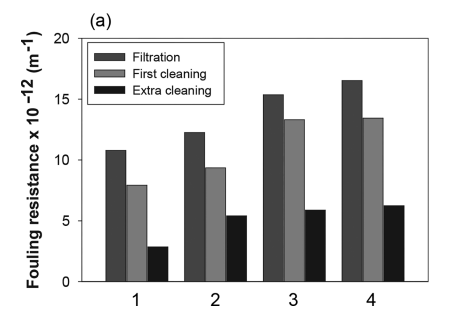
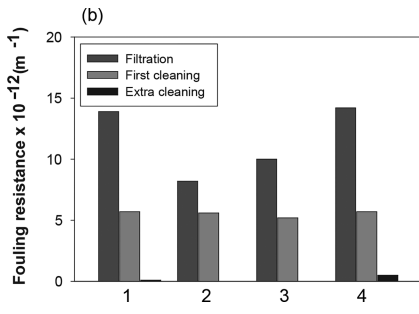


Figure 5. Normalized permeance as a function of permeate volume during consecutive sets of humic acid filtration on PES/PVP blend membrane. Circles, gray stars, and white stars represent normalized permeance during filtration, after the first cleaning and after the extra cleaning, respectively. Vertical, dashed lines indicate the end of a filtration-cleaning period. (a) Humic acid only, with no microgel addition. (b) Humic acid with 0.01 g/L p(NIPAm-co-SBMA) microgels and heating/cooling during cleaning steps. (c) Humic acid with 0.01 g/L p(NIPAm-co-SBMA) microgels with no heating/cooling during cleaning steps. Initial clean membrane pure water permeances are 5.8, 3.4, and 4.4 L/h·m²·bar for (a), (b), and (c), respectively.

sets, however, there was a continuing decline in permeance, indicating irreversible fouling. When p(NIPAm-co-SBMA) microgels were added to the feed during filtration, and temperature switching was used during the cleaning steps, not only was the fouling less, but also the initial permeance could be fully recovered after the extra cleaning step in all four filtration sets (Figure 5(b)). To distinguish the effect of microgel presence from its size change during filtration, a control experiment was done using the microgels in filtration while applying no temperature change during cleaning (Figure 5(c)). The flux decline was again less than the case where no microgel was used, implying a less resistant foulant deposit. However, fouling reversibility after cleaning was less complete, showing that swelling/collapsing behavior of the microgels is effective in fouling removal.





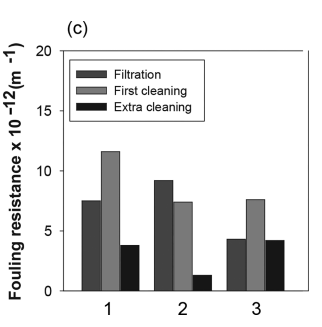
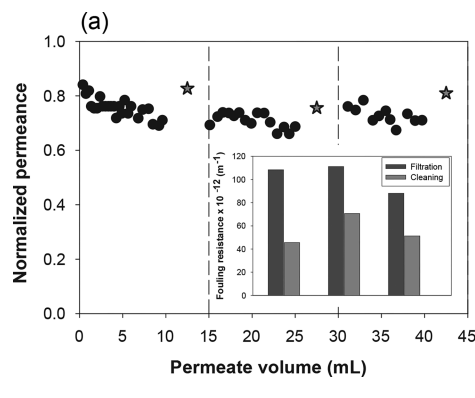


Figure 6. Fouling resistance during filtration, after the first cleaning and after the extra cleaning on PES/PVP blend membrane. (a) Humic acid only, with no microgel addition. (b) Humic acid with 0.01 g/L p(NIPAm-co-SBMA) microgels and heating/cooling during cleaning steps. (c) Humic acid with 0.01 g/L p(NIPAm-co-SBMA) microgels with no heating/cooling during cleaning steps. Numbers 1-4 on the x axes represent consequent filtration-cleaning sets, separated from each other with vertical dashed lines in Figure 5.



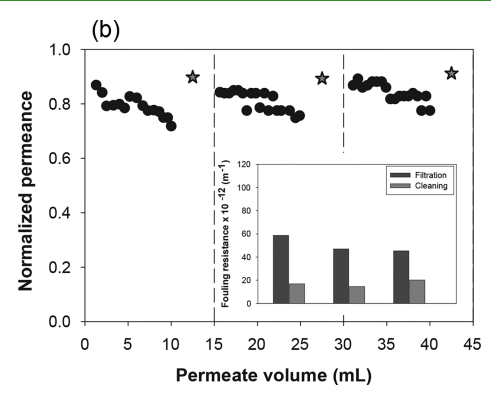


Figure 7. Normalized permeance as a function of permeate volume (circles) and after a single cleaning (gray stars) on PES/PVP blend membrane. Vertical, dashed lines indicate the end of a filtration-cleaning period. (a) Humic acid in 0.5 M NaCl. (b) Humic acid with 0.01 g/L p(NIPAm-coSBMA) microgels in 0.5 M NaCl. Heating applied during cleaning in both. The insets in (a) and (b) show the fouling resistance after filtration and cleaning for the tests without and with microgels, respectively. Initial clean membrane pure water permeances are 1.6 and 2.4 L/h·m²-bar for (a) and (b), respectively.

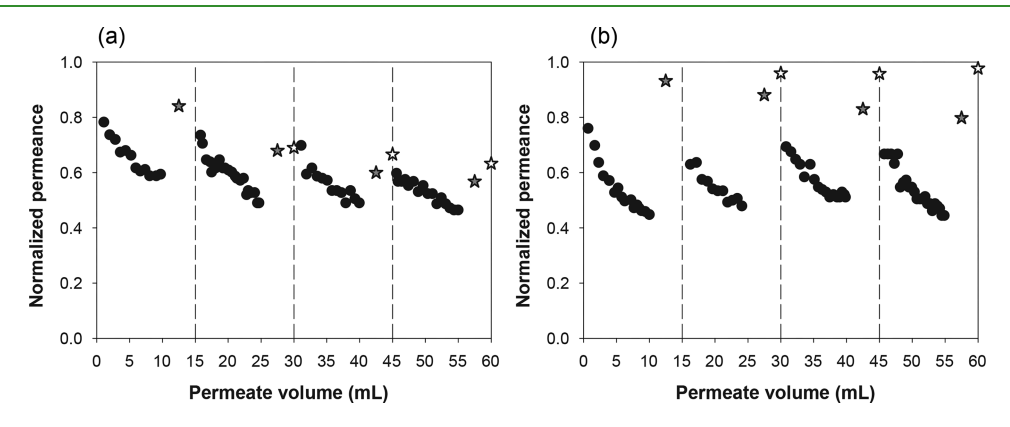
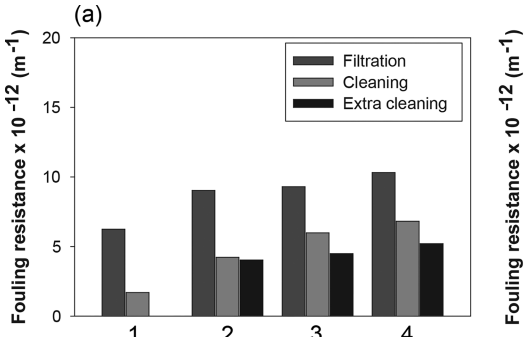


Figure 8. Normalized permeance as a function of permeate volume during four sets of humic acid filtration on PES membrane. Circles, gray stars, and white stars represent normalized permeance during filtration, after the first cleaning, and after the extra cleaning, respectively. Vertical, dashed lines indicate the end of a filtration-cleaning period. (a) Humic acid only, with no microgel addition. (b) Humic acid with 0.01 g/L p(NIPAm-co-SBMA) microgels and heating/cooling during cleaning steps. Initial clean membrane pure water permeances are 39 and 33 L/h·m²-bar for (a) and (b), respectively.

To distinguish effects of different starting permeances on the rate of permeance decline, fouling behavior was also analyzed by the resistance due to fouling at the end of the filtration and the part of this resistance that can be cleaned by temperature switching. Figure 6 shows these resistances for the three cases considered, where it can be seen that fouling removal was significantly more with microgels. After an extra cleaning, about one-third of the fouling resistance still remained on the membrane surface when no microgels were used. With

microgels and temperature change during cleaning, a single cleaning could remove half the fouling resistance, and with extra cleaning, all fouling was removed. When no temperature change was applied during cleaning in the presence of microgels, the extent of fouling resistance removal was quite the same as the case without microgels, confirming that it was the swelling and collapsing behavior of the gels that was effective in cleaning the deposit.

ACS Applied Materials & Interfaces



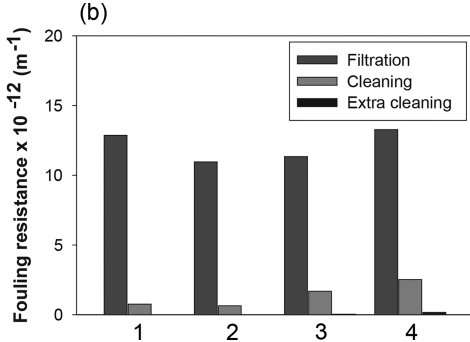


Figure 9. Fouling resistance during filtration, after the first cleaning and after the extra cleaning on PES membrane. (a) Humic acid only, with no microgel addition. (b) Humic acid with 0.01 g/L p(NIPAm-co-SBMA) microgels and heating/cooling during cleaning steps. Numbers 1-4 on the x axes represent consequent filtration-cleaning sets, separated from each other with vertical dashed lines in Figure 8.

The same tests were also carried out with and without p(NIPAm-co-SBMA) microgels in 0.5 M NaCl solution. It was observed that fouling was more severe when there is salt in solution both with and without the microgels. Permeance declined to about 70% of the pure water permeance and the fouling resistance was about an order of magnitude higher than when filtrations were done in pure water (Figure 7). The higher resistance of humic acid fouling layer in the presence of salt can be attributed to the salting out of humic acid at high ionic strength thus allowing a more compact deposit.70 microgels, the fouling resistance was about half the amount with no microgel, which may be due to the highly swollen microgel loosening the foulant layer. While fouling was more severe at high ionic strength both with and without microgels, the percentage of fouling resistance that could be removed with a single cleaning was similar when the use of p(NIPAm-co-SBMA) microgels in pure water and in saline water was compared.

P(NIPAm-co-SBMA) Microgels on PES Membrane. Fouling on PES/PVP blend membranes was relatively low, presumably due to the hydrophilicity of the PVP-enriched surfaces of these membranes.⁵ The higher pure water permeance of the PES membrane is likely another contribution to this difference, since in a constant TMP fouling test, a membrane with a higher initial permeance experiences a higher permeate drag toward the membrane, which makes it foul more in the beginning of the filtration.

The effectiveness of p(NIPAm-co-SBMA) microgels was tested on the more hydrophobic PES membranes, as well. Figure 8 shows the flux decline in four consequent filtration-cleaningextra cleaning steps with and without p(NIPAm-co-SBMA) microgels. In both cases there was a higher permeance decline compared to the PES/PVP blend membranes. When humic acid alone was filtered through the PES membrane, the permeance was about 60% of the pure water permeance of the clean membrane when the first 10 mL permeate was taken. This could only be increased up to 85% with cleaning and in the second 10 mL filtration, it declined to 60% of this starting value. After cleaning the permeance increased to 68% of the clean membrane pure water permeance and was marginally improved with extra cleaning. In subsequent filtrations the permeance decline followed a similar trend and the fouling could only be cleaned to a certain extent with 40% of the clean membrane permeance lost after four filtration-cleaning steps.

When 0.01 g/L p(NIPAm-co-SBMA) was added to the feed solution, the permeance decline was higher. The permeance at the end of filtration was, on average, 45% of the starting permeance. This fouling, however could be fully removed with

cleaning. In the first cleaning, about 85% of the initial permeance was recovered and after an extra cleaning essentially all fouling was removed.

The same can be observed when comparing the fouling resistance data (Figure 9). While, there exists a higher fouling resistance when microgels were used, 90% of the fouling resistance was cleaned with a single cleaning and about 100% was cleaned after the extra cleaning. On the other hand, without the microgels, about half the fouling resistance remained after the first as well as the extra cleaning.

Figure 10 shows the photographs of these membranes after the first and extra cleaning steps. It is clearly seen that the

	HA + C	CaCl ₂	HA + CaCl ₂ + P(NIPAm-co-SBMA)		
	1 st cleaning	extra cleaning	1 st cleaning	extra cleaning	
1		х		х	
2					
3					
4					

Figure 10. Photographs of PES membranes after the first (first and third columns) and extra (second and fourth columns) cleaning steps.

microgels could effectively clean the foulant deposit from the membrane surface, even with a single cleaning step, whereas without them, a significant amount of humic acid deposit remained on the membrane surface.

Effect of Fouling Resistance on Subsequent Cleanability. When fouling tests are done by challenging the membranes to be compared with the same permeate volume, the fouling resistance ending up on the membrane can be different, which in turn challenges the cleaning procedure with different resistances to remove from the membrane surface. To compare the effect of microgels on cleaning the same amount of **ACS Applied Materials & Interfaces**

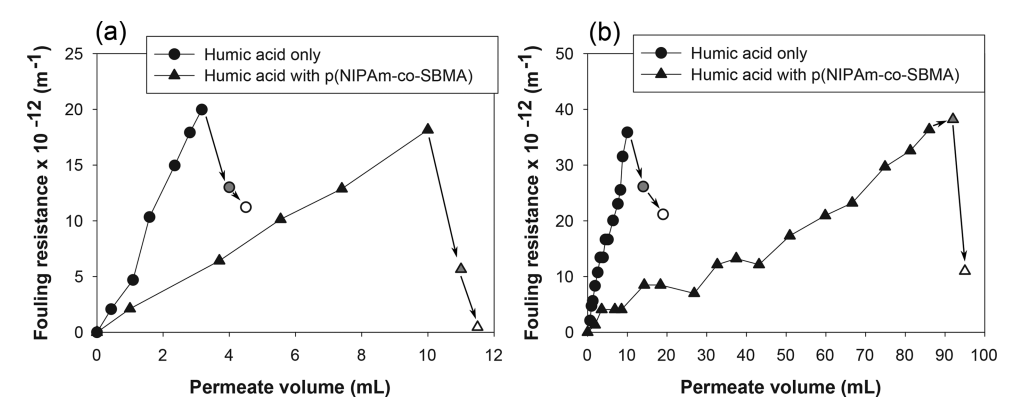


Figure 11. Comparison of fouling reversibilty with and without p(NIPAm-co-SBMA) microgels after filtration until a (a) low fouling resistance and (b) high fouling resistance was obtained. Black filled symbols show the fouling resistance during filtration, gray symbols show the fouling resistance after the first cleaning, and white symbols show the fouling resistance after the extra cleaning.

fouling resistance, we have done filtrations until a low fouling resistance $(20 \times 10^{12} \text{ m}^{-1})$ and a high fouling resistance $(35 \times 10^{12} \text{ m}^{-1})$ 10¹² m⁻¹) with and without the p(NIPAm-co-SBMA) microgels, and subjected the membranes to the same cleaning with an extra cleaning procedure.

Figure 11(a) shows the membranes challenged with a low fouling resistance with and without microgels. This resistance could be fully removed when microgels are used, whereas about half of it was irreversible without the microgels. Similarly, when the filtration was continued until a higher fouling resistance built up on the membrane, about 60% of the resistance remained on the membrane without the use of microgels, whereas only 30% of the resistance was irreversible when microgels were used.

CONCLUSIONS

p(NIPAm) and p(NIPAm-co-SBMA) microgels were synthesized by free radical precipitation polymerization and were used to remove fouling layers from membrane surfaces with their size change upon changing temperature following their deposition on the surface together with foulants. This was, to our knowledge, the first attempt at using responsive microgels not as membrane materials, but as feed additives to modulate the removability of a cake layer.

p(NIPAm) microgels were not effective in removing humic acid foulant deposits, possibly due to interactions between p(NIPAm) and humic acids preventing the swelling of the microgel within the deposit. P(NIPAm-co-SBMA) microgels, on the other hand, could fully clean foulant deposits on PES/PVP membranes with a cleaning procedure of switching the temperature above, below, and above the LCST, as opposed to the absence of microgels as well as the absence of a temperature change when microgels were present in the feed. They were also effective in removing the fouling in 0.5 M NaCl medium. Fouling of PES membranes, which was significantly more than PES/PVP membranes, could also be cleaned completely as observed from the membranes' filtration performance as well as the appearance of the membranes before and after cleaning. Finally, membranes were challenged with a low and high fouling resistance with and without p(NIPAm-co-SBMA) microgels, to assess the effectiveness of microgels' stimulus response against the same fouling resistance, where it was also observed that fouling reversibility was higher with the use of microgels and a temperature switching method for cleaning. The method presented is a practical way of cleaning cake fouling,

which can easily be implemented in existing membrane processes.

AUTHOR INFORMATION

Corresponding Author

*E-mail: zculfaz@metu.edu.tr.

Ayse Asatekin: 0000-0002-4704-1542

P. Zeynep Culfaz-Emecen: 0000-0002-9609-5256

Notes

The authors declare no competing financial interest.

ACKNOWLEDGMENTS

We thank TUBITAK MAG 116M047, NSF CBET 1437772, and Middle East Technical University Research Fund BAP-03-04-2017-001 for financial support.

REFERENCES

- (1) Gao, W.; Liang, H.; Ma, J.; Han, M.; Chen, Z.-L.; Han, Z.-S.; Li, G.-B. Membrane fouling control in ultrafiltration technology for drinking water production: A review. Desalination 2011, 272, 1-8.
- (2) Jermann, D.; Pronk, W.; Meylan, S.; Boller, M. Interplay of different NOM fouling mechanisms during ultrafiltration for drinking water production. Water Res. 2007, 41, 1713-1722.
- (3) Katsoufidou, K.; Yiantsios, S.; Karabelas, A. A study of ultrafiltration membrane fouling by humic acids and flux recovery by backwashing: Experiments and modeling. J. Membr. Sci. 2005, 266, 40-
- (4) Hwang, K.-J.; Sz, P.-Y. Membrane fouling mechanism and concentration effect in cross-flow microfiltration of BSA/dextran mixtures. Chem. Eng. J. 2011, 166, 669-677.
- (5) Wienk, I.; Olde Scholtenhuis, F.; van den Boomgaard, T.; Smolders, C. Spinning of hollow fiber ultrafiltration membranes from a polymer blend. J. Membr. Sci. 1995, 106, 233-243.
- (6) Asatekin, A.; Kang, S.; Elimelech, M.; Mayes, A. Anti-fouling ultrafiltration membranes containing polyacrylonitrile-graft-poly-(ethylene oxide) comb copolymer additives. J. Membr. Sci. 2007, 298, 136-146.
- (7) Susanto, H.; Ulbricht, M. Characteristics, performance and stability of polyethersulfone ultrafiltration membranes prepared by phase separation method using different macromolecular additives. J. Membr. Sci. 2009, 327, 125-135.
- (8) Wang, Y.-Q.; Wang, T.; Su, Y.-L.; Peng, F.-B.; Wu, H.; Jiang, Z.-Y. Remarkable reduction of irreversible fouling and improvement of the permeation properties of poly(ether sulfone) ultrafiltration membranes by blending with pluronic F127. Langmuir 2005, 21, 11856-11862.

- (9) Hester, J.; Mayes, A. Design and performance of foul-resistant poly(vinylidene fluoride) membranes prepared in a single-step by surface segregation. J. Membr. Sci. 2002, 202, 119-135.
- (10) Kaner, P.; Rubakh, E.; Kim, D.; Asatekin, A. Zwitterioncontaining polymer additives for fouling resistant ultrafiltration membranes. J. Membr. Sci. 2017, 533, 141-159.
- (11) Susanto, H.; Ulbricht, M. Photografted thin polymer hydrogel layers on PES ultrafiltration membranes: characterization, stability, and influence on separation performance. Langmuir 2007, 23, 7818-7830.
- (12) Chiang, Y.-C.; Chang, Y.; Higuchi, A.; Chen, W.-Y.; Ruaan, R.-C. Sulfobetaine-grafted poly(vinylidene fluoride) ultrafiltration membranes exhibit excellent antifouling property. J. Membr. Sci. 2009, 339, 151-159.
- (13) McCloskey, B.; Park, H.; Ju, H.; Rowe, B.; Miller, D.; Freeman, B. A bioinspired fouling-resistant surface modification for water purification membranes. J. Membr. Sci. 2012, 413-414, 82-90.
- (14) Asatekin, A.; Menniti, A.; Kang, S.; Elimelech, M.; Morgenroth, E.; Mayes, A. Antifouling nanofiltration membranes for membrane bioreactors from self-assembling graft copolymers. J. Membr. Sci. 2006, 285, 81-89.
- (15) Chen, W.; Su, Y.; Zheng, L.; Wang, L.; Jiang, Z. The improved oil/water separation performance of cellulose acetate-graft-polyacrylonitrile membranes. J. Membr. Sci. 2009, 337, 98-105.
- (16) Asatekin, A.; Olivetti, E.; Mayes, A. Fouling resistant, high flux nanofiltration membranes from polyacrylonitrile-graft-poly(ethylene oxide). J. Membr. Sci. 2009, 332, 6-12.
- (17) Bengani, P.; Kou, Y.; Asatekin, A. Zwitterionic copolymer selfassembly for fouling resistant, high flux membranes with size-based small molecule selectivity. J. Membr. Sci. 2015, 493, 755-765.
- (18) Bengani-Lutz, P.; Converse, E.; Cebe, P.; Asatekin, A. Self-Assembling Zwitterionic Copolymers as Membrane Selective Layers with Excellent Fouling Resistance: Effect of Zwitterion Chemistry. ACS Appl. Mater. Interfaces 2017, 9, 20859-20872.
- (19) Pendashteh, A. R.; Fakhru'l-Razi, A.; Madaeni, S. S.; Abdullah, L. C.; Abidin, Z. Z.; Biak, D. R. A. Membrane foulants characterization in a membrane bioreactor (MBR) treating hypersaline oily wastewater. Chem. Eng. J. 2011, 168, 140-150.
- (20) Lee, J.; Ahn, W.-Y.; Lee, C.-H. Comparison of the filtration characteristics between attached and suspended growth microorganisms in submerged membrane bioreactor. Water Res. 2001, 35, 2435-2445.
- (21) Jacquin, C.; Teychene, B.; Lemee, L.; Lesage, G.; Heran, M. Characteristics and fouling behaviors of Dissolved Organic Matter fractions in a full-scale submerged membrane bioreactor for municipal wastewater treatment. Biochem. Eng. J. 2018, 132, 169-181.
- (22) Tay, M. F.; Liu, C.; Cornelissen, E. R.; Wu, B.; Chong, T. H. The feasibility of nanofiltration membrane bioreactor (NF-MBR)+reverse osmosis (RO) process for water reclamation: Comparison with ultrafiltration membrane bioreactor (UF-MBR)+RO process. Water Res. 2018, 129, 180-189.
- (23) Bugge, T. V.; Jørgensen, M. K.; Christensen, M. L.; Keiding, K. Modeling cake buildup under TMP-step filtration in a membrane bioreactor: Cake compressibility is significant. Water Res. 2012, 46,
- (24) Maqbool, T.; Khan, S. J.; Lee, C.-H. Effects of filtration modes on membrane fouling behavior and treatment in submerged membrane bioreactor. Bioresour. Technol. 2014, 172, 391-395.
- (25) van der Marel, P.; Zwijnenburg, A.; Kemperman, A.; Wessling, M.; Temmink, H.; van der Meer, W. An improved flux-step method to determine the critical flux and the critical flux for irreversibility in a membrane bioreactor. J. Membr. Sci. 2009, 332, 24-29.
- (26) Wu, J.; Le-Clech, P.; Stuetz, R. M.; Fane, A. G.; Chen, V. Effects of relaxation and backwashing conditions on fouling in membrane bioreactor. J. Membr. Sci. 2008, 324, 26-32.
- (27) Le-Clech, P.; Chen, V.; Fane, T. A. Fouling in membrane bioreactors used in wastewater treatment. J. Membr. Sci. 2006, 284, 17-53.

- (28) Chen, J.; Kim, S.; Ting, Y. Optimization of membrane physical and chemical cleaning by a statistically designed approach. J. Membr. Sci. 2003, 219, 27-45.
- (29) Katsoufidou, K.; Yiantsios, S.; Karabelas, A. Experimental study of ultrafiltration membrane fouling by sodium alginate and flux recovery by backwashing. J. Membr. Sci. 2007, 300, 137-146.
- (30) Zsirai, T.; Buzatu, P.; Aerts, P.; Judd, S. Efficacy of relaxation, backflushing, chemical cleaning and clogging removal for an immersed hollow fibre membrane bioreactor. Water Res. 2012, 46, 4499-4507.
- (31) Hong, S.; Bae, T.; Tak, T.; Hong, S.; Randall, A. Fouling control in activated sludge submerged hollow fiber membrane bioreactors. Desalination 2002, 143, 219-228.
- (32) Zhang, K.; Cui, Z.; Field, R. Effect of bubble size and frequency on mass transfer in flat sheet MBR. J. Membr. Sci. 2009, 332, 30-37.
- (33) Wibisono, Y.; Cornelissen, E.; Kemperman, A.; Van Der Meer, W.; Nijmeijer, K. Two-phase flow in membrane processes: A technology with a future. J. Membr. Sci. 2014, 453, 566-602.
- (34) Kim, J.-S.; Lee, C.-H.; Chun, H.-D. Comparison of ultrafiltration characteristics between activated sludge-and BAC sludge. Water Res. 1998, 32, 3443-3451.
- (35) Loulergue, P.; Weckert, M.; Reboul, B.; Cabassud, C.; Uhl, W.; Guigui, C. Mechanisms of action of particles used for fouling mitigation in membrane bioreactors. Water Res. 2014, 66, 40-52.
- (36) Scannapieco, D.; Naddeo, V.; Belgiorno, V. Control of fouling in MBRs through nanospheres addition. Desalin. Water Treat. 2015, 55, 702-711.
- (37) Barth, M.; Wiese, M.; Ogieglo, W.; Go, D.; Kuehne, A.; Wessling, M. Monolayer microgel composite membranes with tunable permeability. J. Membr. Sci. 2018, 555, 473-482.
- (38) Chen, Y.-C.; Xie, R.; Chu, L.-Y. Stimuli-responsive gating membranes responding to temperature, pH, salt concentration and anion species. J. Membr. Sci. 2013, 442, 206-215.
- (39) Hilke, R.; Pradeep, N.; Madhavan, P.; Vainio, U.; Behzad, A.; Sougrat, R.; Nunes, S.; Peinemann, K.-V. Block copolymer hollow fiber membranes with catalytic activity and pH-response. ACS Appl. Mater. Interfaces 2013, 5, 7001-7006.
- (40) Li, J.-J.; Zhou, Y.-N.; Luo, Z.-H. Smart Fiber Membrane for pH-Induced Oil/Water Separation. ACS Appl. Mater. Interfaces 2015, 7, 19643-19650.
- (41) Liu, H.; Liao, J.; Zhao, Y.; Sotto, A.; Zhu, J.; van der Bruggen, B.; Gao, C.; Shen, J. Bioinspired dual stimuli-responsive membranes with enhanced gating ratios and reversible performances for water gating. J. Membr. Sci. 2018, 564, 53-61.
- (42) Liu, H.; Zhao, X.; Jia, N.; Sotto, A.; Zhao, Y.; Shen, J.; Gao, C.; Van Der Bruggen, B. Engineering of thermo-/pH-responsive membranes with enhanced gating coefficients, reversible behaviors and self-cleaning performance through acetic acid boosted microgel assembly. J. Mater. Chem. A 2018, 6, 11874-11883.
- (43) Lohaus, T.; de Wit, P.; Kather, M.; Menne, D.; Benes, N.; Pich, A.; Wessling, M. Tunable permeability and selectivity: Heatable inorganic porous hollow fiber membrane with a thermo-responsive microgel coating. J. Membr. Sci. 2017, 539, 451-457.
- (44) Menne, D.; Pitsch, F.; Wong, J.; Pich, A.; Wessling, M. Temperature-modulated water filtration using microgel-functionalized hollow-fiber membranes. Angew. Chem., Int. Ed. 2014, 53, 5706-5710.
- (45) Schacher, F.; Rudolph, T.; Wieberger, F.; Ulbricht, M.; Müller, A. Double stimuli-responsive ultrafiltration membranes from polystyreneblock-poly(N, N -dimethylaminoethyl methacrylate) diblock copolymers. ACS Appl. Mater. Interfaces 2009, 1, 1492-1503.
- (46) Xie, R.; Li, Y.; Chu, L.-Y. Preparation of thermo-responsive gating membranes with controllable response temperature. J. Membr. Sci. 2007, 289, 76-85.
- (47) Zhao, Y.-H.; Wee, K.-H.; Bai, R. A novel electrolyte-responsive membrane with tunable permeation selectivity for protein purification. ACS Appl. Mater. Interfaces 2010, 2, 203-211.
- (48) Meng, J.; Cao, Z.; Ni, L.; Zhang, Y.; Wang, X.; Zhang, X.; Liu, E. A novel salt-responsive TFC RO membrane having superior antifouling and easy-cleaning properties. J. Membr. Sci. 2014, 461, 123-129.

- (49) Mondal, S.; Wickramasinghe, S. Photo-induced graft polymerization of N-isopropyl acrylamide on thin film composite membrane: Produced water treatment and antifouling properties. *Sep. Purif. Technol.* **2012**, *90*, 231–238.
- (50) Wandera, D.; Wickramasinghe, S. R.; Husson, S. M. Modification and characterization of ultrafiltration membranes for treatment of produced water. *J. Membr. Sci.* **2011**, *373*, 178–188.
- (51) You, M.; Wang, P.; Xu, M.; Yuan, T.; Meng, J. Fouling resistance and cleaning efficiency of stimuli-responsive reverse osmosis (RO) membranes. *Polymer* **2016**, *103*, 457–467 New Polymeric Materials and Characterization Methods for Water Purification.
- (52) Zhang, X.; Tian, J.; Gao, S.; Shi, W.; Zhang, Z.; Cui, F.; Zhang, S.; Guo, S.; Yang, X.; Xie, H.; Liu, D. Surface functionalization of TFC FO membranes with zwitterionic polymers: Improvement of antifouling and salt-responsive cleaning properties. *J. Membr. Sci.* **2017**, *544*, 368–377.
- (53) Zhao, Y.; Zhou, S.; Li, M.; Xue, A.; Zhang, Y.; Wang, J.; Xing, W. Humic acid removal and easy-cleanability using temperature-responsive ZrO2 tubular membranes grafted with poly(N-isopropylacrylamide) brush chains. *Water Res.* **2013**, *47*, 2375–2386.
- (54) Zhou, S.; Xue, A.; Zhang, Y.; Li, M.; Wang, J.; Zhao, Y.; Xing, W. Fabrication of temperature-responsive ZrO2 tubular membranes, grafted with poly (N-isopropylacrylamide) brush chains, for protein removal and easy cleaning. *J. Membr. Sci.* **2014**, *450*, 351–361.
- (55) Chede, S.; Escobar, I. Fouling control using temperature responsive N-isopropylacrylamide (NIPAAm) membranes. *Environ. Prog. Sustainable Energy* **2016**, 35, 416–427 cited By 5. .
- (56) Kaner, P.; Hu, X.; Thomas, S.; Asatekin, A. Self-Cleaning Membranes from Comb-Shaped Copolymers with Photoresponsive Side Groups. ACS Appl. Mater. Interfaces 2017, 9, 13619–13631 cited By 8.
- (57) Xu, L. L.; Xu, Y.; Liu, L.; Wang, K. P.; Patterson, D. A.; Wang, J. Electrically responsive ultrafiltration polyaniline membrane to solve fouling under applied potential. *J. Membr. Sci.* **2019**, 572, 442–452.
- (58) Zhao, X.; Liu, C. Efficient preparation of a novel PVDF antifouling membrane based on the solvent-responsive cleaning properties. *Sep. Purif. Technol.* **2019**, 210, 100–106.
- (59) Ramanan, S. N.; Shahkaramipour, N.; Tran, T.; Zhu, L.; Venna, S. R.; Lim, C.-K.; Singh, A.; Prasad, P. N.; Lin, H. Self-cleaning membranes for water purification by co-deposition of photo-mobile 4,4-azodianiline and bio-adhesive polydopamine. *J. Membr. Sci.* **2018**, 554, 164–174.
- (60) Yu, S.; Lü, Z.; Chen, Z.; Liu, X.; Liu, M.; Gao, C. Surface modification of thin-film composite polyamide reverse osmosis membranes by coating N-isopropylacrylamide-co-acrylic acid copolymers for improved membrane properties. *J. Membr. Sci.* **2011**, *371*, 293–306
- (61) Yu, S.; Chen, Z.; Liu, J.; Yao, G.; Liu, M.; Gao, C. Intensified cleaning of organic-fouled reverse osmosis membranes by thermoresponsive polymer (TRP). *J. Membr. Sci.* **2012**, 392–393, 181–191.
- (62) Liu, Y.; Koops, G.; Strathmann, H. Characterization of morphology controlled polyethersulfone hollow fiber membranes by the addition of polyethylene glycol to the dope and bore liquid solution. *J. Membr. Sci.* **2003**, 223, 187–199.
- (63) Susanto, H.; Stahra, N.; Ulbricht, M. High performance polyethersulfone microfiltration membranes having high flux and stable hydrophilic property. *J. Membr. Sci.* **2009**, 342, 153–164.
- (64) Katsoufidou, K.; Sioutopoulos, D.; Yiantsios, S.; Karabelas, A. UF membrane fouling by mixtures of humic acids and sodium alginate: Fouling mechanisms and reversibility. *Desalination* **2010**, *264*, 220–227.
- (65) Schafer, A.; Fane, A.; Waite, T. Nanofiltration of natural organic matter: removal, fouling and the influence of multivalent ions. *Desalination* **1998**, *118*, 109–122.
- (66) Pelton, R. Temperature-sensitive aqueous microgels. *Adv. Colloid Interface Sci.* **2000**, *85*, 1–33.
- (67) Lu, Y.; Zhou, K.; Ding, Y.; Zhang, G.; Wu, C. Origin of hysteresis observed in association and dissociation of polymer chains in water. *Phys. Chem. Chem. Phys.* **2010**, *12*, 3188–3194.

- (68) Maeda, Y.; Nakamura, T.; Ikeda, I. Changes in the hydration states of poly(N-alkylacrylamide)s during their phase transitions in water observed by FTIR spectroscopy. *Macromolecules* **2001**, *34*, 1391–1399
- (69) Schild, H. Poly(N-isopropylacrylamide): experiment, theory and application. *Prog. Polym. Sci.* **1992**, *17*, 163–249.
- (70) Hong, S.; Elimelech, M. Chemical and physical aspects of natural organic matter (NOM) fouling of nanofiltration membranes. *J. Membr. Sci.* 1997, 132, 159–181.